iScience

CellPress
OPEN ACCESS

Article

Optimizing the growth of *Haematococcus pluvialis* based on a novel microbubble-driven photobioreactor

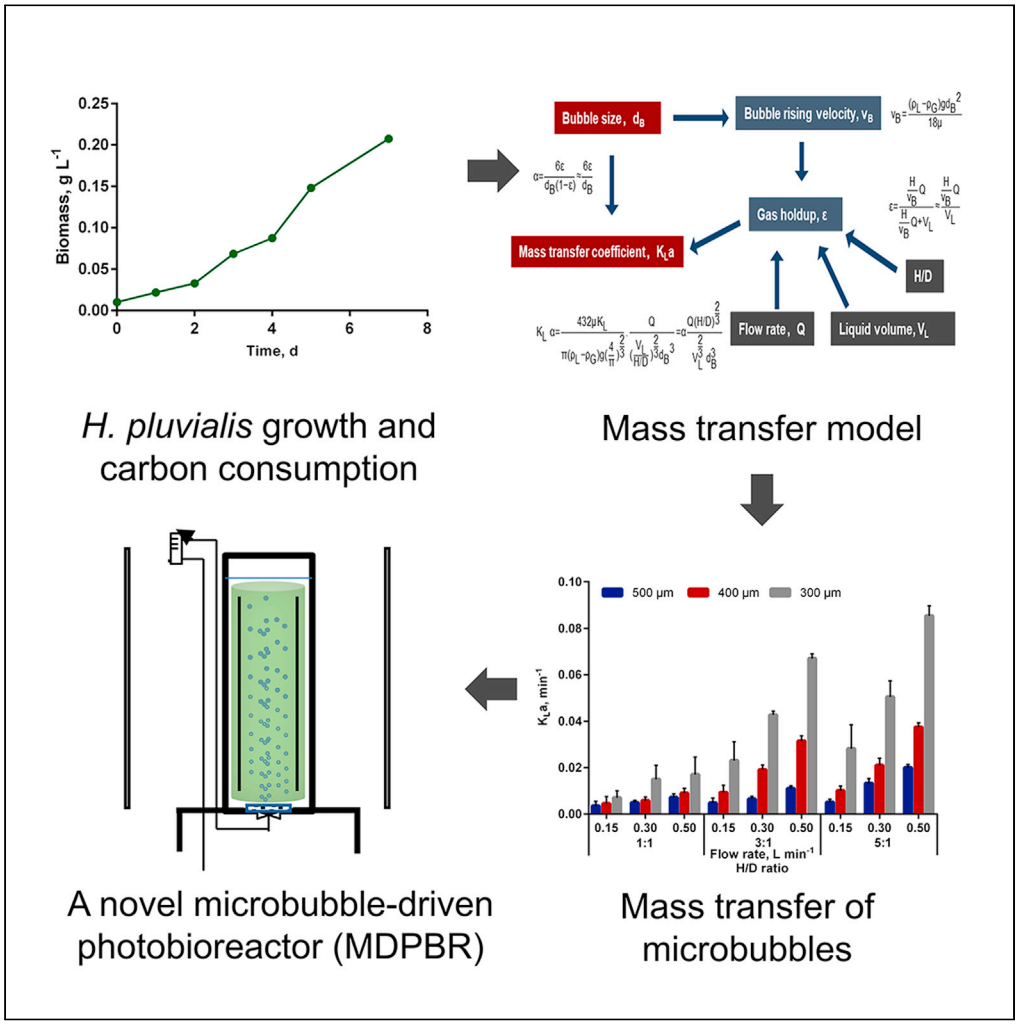

Kebi Wu, Kezhen Ying, Jin Zhou, ..., James Hanotu, Xiaoshan Zhu, Zhonghua Cai

caizh@sz.tsinghua.edu.cn

Highlights

The CO_2 mass transfer demand for optimal *H. pluvialis* growth is identified

The impact of key parameters on mass transfer are discussed

Reducing bubble size has pronounced effect on CO_2 mass transfer

Microbubble photobioreactor demonstrates a high biomass of *H. pluvialis*

Wu et al., iScience *24*, 103461
December 17, 2021
https://doi.org/10.1016/j.isci.2021.103461

iScience

CellPress
OPEN ACCESS

Article

Optimizing the growth of *Haematococcus pluvialis* based on a novel microbubble-driven photobioreactor

Kebi Wu,[1,2,6] Kezhen Ying,[2,5,6] Jin Zhou,[2] Dai Liu,[2] Lu Liu,[1,2] Yi Tao,[3] James Hanotu,[4] Xiaoshan Zhu,[2] and Zhonghua Cai[1,2,7,*]

SUMMARY

***Haematococcus pluvialis*, the richest bioresource for natural astaxanthin, encounters a challenge of achieving high growth rate when it comes to mass biomass production. Based on the substrate consumption model and Redfield ratio, rapid algae growth benefits from a proper carbon supply. However, the conventional cultivation schemes with limited carbon dioxide (CO_2) supply and inefficient carbon mass transfer could have constrained the carbon capture and growing ability of *H. pluvialis*. We hypothesize that optimal *H. pluvialis* growth improvement may be achieved by efficient CO_2 supply. Here, in this study, we first identified the carbon consumption of *H. pluvialis* during exponential growth. Then, a novel microbubble-driven photobioreactor (MDPBR) was designed to satisfy the carbon demand. The novel microbubble photobioreactor improves the CO_2 supply by reducing bubble size, significantly elevating the CO_2 mass transfer. With only 0.05 L min^{-1} of gas flow rate, higher cell growth rate (0.49 d^{-1}) has been achieved in MDPBR.**

INTRODUCTION

Microalgae *Haematococcus pluvialis* (*H. pluvialis*) is considered to be the richest bioresource of astaxanthin (Ambati et al., 2014; Kaewpintong et al., 2007). Astaxanthin ($C_{40}H_{52}O_4$, 3,3′-dihydroxy-β,β′-carotene-4,4′-dione) gains its name as a potent antioxidant, widely applied for anti-inflammation, anti-aging, immune system enhancement, cancer prevention, etc., (Fakhri et al., 2020; Kim et al., 2019; Medhi and Kalita, 2021). Involving astaxanthin in diet can significantly reduce MCP-1, TNF-α, IL-6, and ROS in diabetic rats (Chan et al., 2012). Recently, algal-derived astaxanthin has been considered as a potential supplementary medicine for clinical trial against COVID-19 for its anti-oxidative benefit (Talukdar et al., 2020). Consequently, there is a rising interest in developing the bioprocess for *H. pluvialis* cultivation.

During the cultivation process, *H. pluvialis* has two distinctive morphologies–green vegetative cell and red rest cell (Xi et al., 2016). Thus, research communities and industries have mainly resorted to two-stage cultural mode, to obtain high biomass and astaxanthin yield (Oslan et al., 2021). During the first stage, cells continuously divide and proliferate. Therefore, full nutrient medium and moderate light intensity, temperature and pH are required (Aflalo et al., 2007; Panis and Carreon, 2016). The second stage refers to a red, non-motile resting stage, when cell division stops and astaxanthin content increases. The harvest of *H. pluvialis* vegetative cells was exposed to stress conditions like high irradiance and acetate addition to accumulate astaxanthin (Sarada et al., 2002).

Achieving a high vegetative cell density in a short period of time before being subjected to the stress conditions is a time-saving and cost-effective way to attain high astaxanthin production (Khoo et al., 2019; Nagappan et al., 2019). Although progress has been made in vegetative *H. pluvialis* cultivation, rapidly achieving high biomass during massive cultivation in vegetative stage remains a challenge and most of the photobioreactor (PBR) cultures have been facing the obstacle of low yield/cost ratio (Colusse et al., 2021; Le-Feuvre et al., 2020).

As *H. pluvialis* is a light sensitive species (Kaewpintong et al., 2007), the key solution to this difficulty could lie in efficient nutrient supply. Base on Monod equation (Kampen et al., 2014):

[1]School of Life Sciences, Tsinghua University, Beijing 100086, China

[2]Shenzhen Public Platform for Screening and Application of Marine Microbial Resources, Shenzhen International Graduate School, Tsinghua University, Shenzhen 518055, China

[3]Guangdong Provincial Engineering Research Centre for Urban Water Recycling and Environmental Safety, Shenzhen International Graduate School, Tsinghua University, Shenzhen 518055, China

[4]Department of Chemical and Biological Engineering, The University of Sheffield, Sheffield S13JD, UK

[5]Oasis Photobio Tech Ltd, Overseas Chinese Scholars Venture Building, South District of High-Tech Industrial Park, Shenzhen, China

[6]These two authors contributed equally

[7]Lead contact

*Correspondence: caizh@sz.tsinghua.edu.cn

https://doi.org/10.1016/j.isci.2021.103461

$$\mu = \mu_{max}\left(\frac{C}{C + K_C}\right) \quad \text{Equation 1}$$

where μ is specific growth rate, d^{-1} defined as (1/X) (dx/dt), μ_{max} is maximum value of μ, d^{-1}, K_C is saturation constant, g L^{-1} at $\mu_{max/2}$, and C is substrate concentration, g L^{-1}, where sufficient substrate supply is closely related to algal specific growth rate (μ). The chemical formations of algae partly determine the nutrient demand (Hillebrand and Sommer, 1999). Previous studies have focused more on nitrogen (N) and phosphor (P) requirements in the cultivation of *H. pluvialis* (Nahidian et al., 2018; Zhao et al., 2020). Tocquin et al. declared that a lower N/P ratio (below 1) favors vegetative growth of *H. pluvialis* (Tocquin et al., 2012), whereas Ding et al. suggested that *H. pluvialis* had relatively low P uptake efficiency (about 99.5 ± 10.1 nmol mg^{-1} Chl a) in both long-term and short-term P uptake experiments (Ding et al., 2019). The inconsistent results indicated that N, P or N/P ratio supplement in medium may not be the sole key parameter of *H. pluvialis* mass production. Meanwhile, the research on carbon supply and consumption of *H. pluvialis* are relatively underexplored (Judd et al., 2017).

Generally, it is believed that the ideal chemical elements present in average phytoplankton biomass demonstrate a Redfield ratio (C: N: P = 106: 16: 1) (Redfield et al., 1963). The idealized chemical reaction of phytoplankton can be illustrated as followed equation (Perdue, 2009; Redfield et al., 1963):

$$106\ CO_2 + 16\ HNO_3 + H_3PO_4 + 78\ H_2O \rightleftharpoons (C_{106}H_{175}O_{42}N_{16}P) + 150\ O_2 \quad \text{Equation 2}$$

which indicates the significance of carbon supply on the growth of phytoplankton. For *H. pluvialis*, the element stoichiometry was reported as 45.6% C, 8.2% H, 6% N, and 0.58% (García-Malea et al., 2006; Razon, 2011), revealing sufficient carbon supply is pivotal for algae biomass enhancement.

Efforts have been made for carbon supply in culture. Carbon supply can be performed under three modes: heterotrophic, mixotrophic, and autotrophic. Heterotrophic cultivation results in low cell concentration, indicating the essentiality of light for high vegetative cell content (Kang et al., 2005). In that case, mixotrophic seems to be a promising method. However, addition of organic carbon source like sodium acetate introduces risk of contamination from other organisms, which could lead to slow growth and even the death of *H. pluvialis* (Pang and Chen, 2017). In addition, autotrophic pre-culture before organic carbon sources addition allows a better performance for cell growth and astaxanthin accumulation (Panutai et al., 2017; Wang et al., 2021). One reason could be that high cell density exhausts the nutrients in the medium which in turn minimizes bacteria contamination (Wen et al., 2020). Thus, autotrophic culture to reach a relatively high biomass is essential for both further mixotrophic culture or astaxanthin induction.

Inorganic carbon supply is crucial for photoautotrophic culture. Carbon dioxide (CO_2) and bicarbonate (HCO_3^-) is considered as the ideal carbon supply. To meet the carbon demand, it requires a constant addition of carbon in batch or fed-batch manner. Nevertheless, continuous addition of bicarbonate can affect the pH and ion level of the medium, causing stress for cell growth (Agranat, 2007). In contrast, the CO_2 supply with a buffer system can avoid the issue and the bubble device is more adjustable and convenient compared with manual addition.

For microalgae mass cultivation, two common systems are open system and close system. Open systems such as open ponds merit flexibility and cost-effective design but suffer CO_2 loss and cell sedimentation (Jerney and Spilling, 2020). Given those issues, PBR, defined as a closed system, was designed. PBRs mainly include stirred tank PBRs, tubular PBRs and bubble column PBRs (Gupta et al., 2015). The stirred tank PBRs require mechanical agitation which tends to generate excess heat and cell damage (Kadic and Heindel, 2014). In tubular PBRs, though they have larger gas-receiving surfaces, the main drawback of them is their poor axial mass transfer—there are significant gas gradients along the tubes (Burgess et al., 2011). *H. pluvialis* that cultivated in 4 types of tubular PBRs merely had the specific growth rate range from 0.07 to 0.12 d^{-1} (Lee et al., 2015). Bubble column PBRs are an alternative for the former bioreactors for its low capital cost, high surface area to volume ratio, and satisfactory mass transfer (Gunjal and Ranade, 2016). The maximum biomass productivity of *Spirulina* (1.03 g L^{-1} day^{-1}) was achieved in the bubble column PBR which is significantly higher than race pond (Singh et al., 2016). Nevertheless, sufficient carbon supply remains a challenge for the traditional bubble column PBRs which commonly generate bubble sizes of 3–6 mm (Kazakis et al., 2008). The optimal CO_2 uptake by *Dunaliella salina* photosynthesis could reach up to 0.3×10^{-4} mol L^{-1} min^{-1} (Zimmerman et al., 2011), whereas the CO_2 mass transfer rate of conventional

technologies was in a range of 0.4×10^{-6} - 0.7×10^{-5} mol L^{-1} min^{-1}, far away from meeting the CO_2 demand for *Dunaliella salina* culture (Ying et al., 2013a). Thus, we hypothesize that optimal *H. pluvialis* growth improvement can be achieved by increasing CO_2 mass transfer for efficient CO_2 supply.

To tackle the mass transfer issue, microbubble technology was developed which has been widely applied in wastewater treatment industries (Rehman et al., 2015; Yao et al., 2016). This technology refers to reducing bubble size of gas injection system in order to achieve both higher mass transfer rate and capture efficiency (Ying et al., 2013a).With microbubble device, threefold improvement of mass transfer rate was achieved, the sufficient mixing and gas flow benefits wastewater treatment process (Rehman et al., 2015). The CO_2 mass transfer rate is mainly determined by the volumetric mass transfer coefficient (K_La) and K_La manifests cubic increase by reducing the bubble size (Erickson, 1990). Studies have shown that the CO_2 mass transfer can be significantly elevated by using microbubble technology (Ying et al., 2013b).Cultured in microbubble induced airlift loop bioreactor, the dry biomass of *Dunaliella salina* was increased from 0.0067 g/L to 0.24 g/L (about 35 folds) after 17 days' culture (Zimmerman et al., 2011). Based on the feature of high mass transfer, it is possible to improve the *H. pluvialis* growth by replacing the conventional CO_2 feeding technologies (with bubble size around 3–6 mm) with microbubbles.

In this study, we addressed three major issues: (1) How much is the carbon consumption of *H. pluvialis* during the exponential growth period? (2) How can the bioreactor meet the carbon demand via optimizing the design parameter? (3) How can the theoretical derivations be applied to the microalgae mass production? Based on the results, we designed a novel microbubble-driven photobioreactor (MDPBR) for *H. pluvialis* rapid cultivation. This technology improves the mass transfer in photobioreactor which is crucial for sufficient carbon supply and can be further applied to microalgae mass production.

RESULTS AND DISCUSSION

H. pluvialis growth and carbon consumption

Effect of carbon concentration on carbon consumption and growth of H.pluvialis

We analyzed how the carbon consumption, biomass, and specific growth rate of *H.pluvialis* vary under different carbon concentrations. The data in Figure 1 shows that higher carbon concentration (8 mM) contributions to higher carbon uptake and biomass increase. The total carbon consumption achieved 0.2, 0.4, and 0.6 mM within 1.5 days with the initial carbon addition at 2, 4, 8 mM, respectively, indicating a daily consumption rate of 0.13, 0.26, and 0.40 mM d^{-1} (Figure 1A). Meanwhile, the control groups (containing medium of different carbon concentration without algae) were proved that experimental operation had no significant effect on the carbon concentration decrease, indicating that the content changes were caused by algal consumption (Figure 1C). The contribution of carbon consumption for unit biomass increase was about 7×10^{-3} mol g^{-1} (the slope of each linear regression), which was nearly identical in each group (Figure 1D). In other words, the yield coefficient (142.9 g_{Cell} mol_C^{-1}) remains unaffected with elevating concentration of carbon. It is highly supported by the theoretical assumption that the activities of the enzymes for nutrient assimilation should be constant under a fixed environment including temperature, pH, salinity, etc., (Najafpour, 2015). Hence, the growth of *H.pluvialis* is adjustable subduing in different carbon concentration conditions.

Higher carbon concentration in the culture was found having a positive effect on the *H. pluvialis* biomass. The *H. pluvialis* culture with 2 mM of carbon addition showed the lowest biomass productivity, with the dry weight ascending by 0.033 g L^{-1}; however, in 4 mM and 8 mM group, the biomass increased by 0.059 and 0.064 g L^{-1}, respectively (Figure 1A). Likewise, the highest specific growth rate was observed in the 8 mM carbon addition group, which is around 78% and 15% higher than the 2 mM and 4 mM group in the first 12 h (Figure 1B). Therefore, the 8 mM carbon addition group outperformed other groups regarding biomass and specific growth rate.

The question worth thinking about is whether it will be beneficial with continuous addition of carbon concentration. Firstly, the response to carbon concentration varies slightly in algal species. Increasing the CO_2 concentration from the atmospheric concentration to 2% resulted in a significant improvement in biomass productivity for the cultivation of *Halochlorella rubescens* (Schultze et al., 2015). Likewise, after comparing the growth of *Chlorella sp.* with different CO_2 concentrations ranging from 0.5% to 5.0%, researchers found that the highest cell density was achieved with 5% CO_2 injection (Ryu et al., 2009). However, the results were found opposite in *Dunaliella salina*. The photosynthetic rate decreased slightly by increasing the CO_2 concentration from 2 mM to 8 mM (Ying et al., 2014). Elevating the CO_2 concentration to 20 mM resulted in the

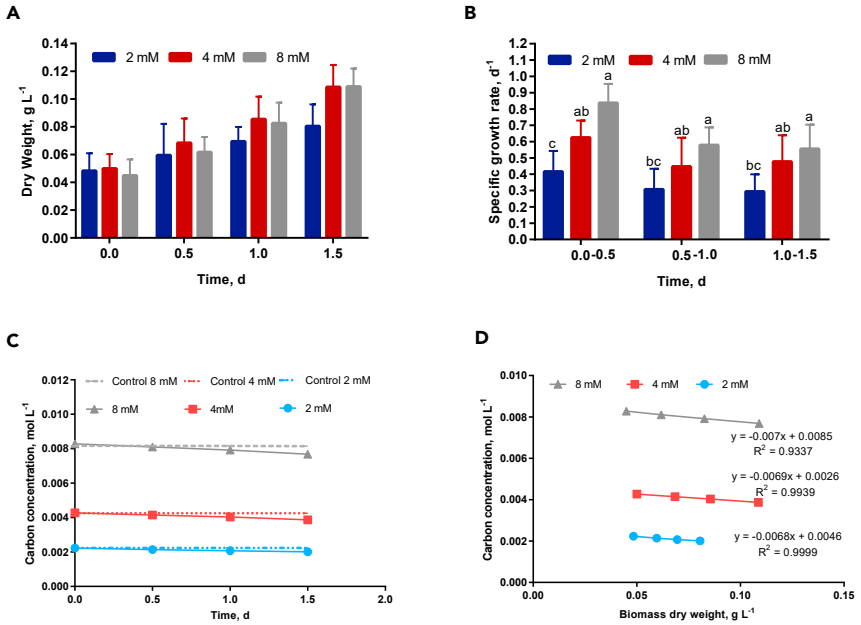

Figure 1. The growths and carbon consumptions of *H. pluvialis* under different carbon concentrations (2 mM, 4 mM and 8 mM)

(A) *H. pluvialis* growth curve.

(B) The overall specific growth rate at each stage of time. Data points are represented as the mean ± standard deviation (SD) for triplicate measurements (n = 3). The different letters indicate a significant difference at $P < 0.05$ level.

(C) Daily carbon concentrations during the cultures. The dotted lines represent the carbon concentrations in the control sets where microalgae were excluded.

(D) Relation between carbon consumption and biomass (dry weight) increases. The slope of the linear regression stands for the carbon consumption per unit of biomass increase.

cell death. Generally, the discrepancy in those results could mainly be attributed to the various levels of tolerance on carbon concentration for various algal species.

Secondly, higher CO_2 concentration could lead to a lower intracellular pH level, which may inhibit the activities of photosynthetic enzymes (Ying et al., 2014). In our case, the pH for each culture was in the range of 7.0–8.0 during the entire experimental period, which was suitable for *H. pluvialis* growth (Choi et al., 2017; Wan et al., 2014). Given the points above, the elevation of carbon concentration should be performed within a proper level.

According to our result, the possible upper limit of carbon concentration in this experimental condition is close to 8 mM. On the one hand, attenuation of the improvement on productivity was observed when rising the carbon concentration from 4 mM to 8 mM. The biomass rises by 78% comparing the 4 mM group with the 2 mM group, but only an 8% increase was shown between 4 mM group and 8 mM group (Figure 1A). Similarly, the descending trend was found in specific growth rates. The value dropped by 0.11, 0.16, and 0.22 d^{-1} of 2 mM, 4 mM, and 8 mM groups, respectively, after cultivation for 36 h. Even though the 8 mM group possesses the greatest specific growth rate, it experiences the greatest μ decline. Based on the Monod model (Equation 1), the instantaneous specific growth rate is positively correlated to the instantaneous concentration of the limiting substrate (carbon concentration in this case). The culture with higher concentration within the tolerant range of carbon supplements leads to a greater μ. Hence, further increase of carbon concentration above the threshold value of 8 mM could result in growth inhibition. Taken together, ascending carbon concentration to a proper level contributes to carbon consumption enhancement and furthermore boosts productivity.

Growth and carbon consumption kinetics

To provide qualified carbon concentration for *H. pluvialis*, we dug deeper into the relationship between growth rate and carbon consumption. The overall specific growth rate for each culture was calculated,

Table 1. List of equations describing the *H. pluvialis* growth and carbon consumption

First order kinetic model for *H. pluvialis* growth and nutrients consumptions

Equations	Representatives
$\frac{dw}{dt} = \mu \cdot w \Rightarrow w = w_0 e^{\mu t}$	Biomass growth, g L^{-1}
$\frac{dC}{dt} = \frac{\mu \cdot w}{Y_{w/C}} = \frac{\mu \cdot w_0 e^{\mu t}}{Y_{w/C}} \Rightarrow \Delta C = \frac{w_0}{Y_{w/C}}(e^{\mu t} - 1)$	Carbon consumption, mol L^{-1} OR g L^{-1}
$\mu = \mu_{max}\left(\frac{C}{C + K_C}\right)$	Specific growth rate under carbon limitation, d^{-1}
$C = C_0 - \Delta C = C_0 - \frac{W_0}{Y_{w/C}}(e^{\mu t} - 1)$	Instantaneous concentration of carbon, mol L^{-1} OR g L^{-1}

Key parameters	Values
μ_{max}	0.68 d^{-1}
Kc	0.002 mol L^{-1} OR 0.024 g L^{-1}
$Y_{w/c}$	142.9 g mol^{-1} OR 11.9 g g^{-1}

whereas the corresponding carbon concentration was estimated as an average value for 1.5 days. The reciprocal of overall specific growth rates ($1/\mu$) versus the reciprocal of carbon concentrations ($1/C_C$) were plotted (data not shown), where the slope and intercept of the linear regression represented the K_C/μ_{max} and $1/\mu_{max}$, respectively, according to the linearized form of Equation 1. The saturation constant on carbon (K_C) and the maximum specific growth rate (μ_{max}) were therefore found to be 2.0 mM and 0.68 d^{-1}, separately. Based on Equation 1, to attain the maximum specific growth rate, the instantaneous carbon concentration in the medium should be maintained at 0.4 M, approximately 200 times higher than K_C (Erickson, 1990). Nonetheless, carbon is commonly provided via CO_2 bubbling for microalgae culture, with the equilibrium carbon concentration of 0.04 M achievable under 100% CO_2 dosing. Therefore, theoretical μ_{max} is hardly achieved in real practice.

The first order kinetic model describing the *H. pluvialis* growth and carbon consumption, including equations and values of the coefficients, was summarized in Table 1. Assuming a) nitrogen and phosphorus are replete and the light limitation does not occur, b) the daily carbon uptake by *H. pluvialis* growth can be traded off by sufficient carbon supplement achieved through 1% CO_2 dosing, and c) the instantaneous concentration of total carbon in the medium is maintained at around 5 mM for the whole culture period, therefore *H. pluvialis* would grow at a constant specific growth rate of 0.49 d^{-1} (about 70% of maximum potential). By using this model, the instantaneous concentration of carbon and biomass for the above experiments were simulated. The computed results were thereafter compared to the experimental results, an identical match was found between them (Figure 2), indicating a strong validity of this model.

The simulation of *H. pluvialis* culture with conventional photobioreactor (with bubble size around 3 mm) was shown in Figure 2. The growth at the first day was estimated according to the equations listed in Table 1. The growth between day 2 and day 7 for the conventional PBR culture was calculated as Equation 3, where W_{t1} and W_{t2} mean the dry weight of biomass at time t_1 and t_2, separately. $\triangle C_{t1,t2}$ represents the overall carbon consumption rate between t_1 and t_2, which is limited to the mass transfer rate of conventional bubbles.

$$W_{t2} = W_{t1} + \frac{\Delta C_{t1,t2}(t_2 - t_1)}{Y_{W/C}} \quad \text{Equation 3}$$

In most of photobioreactor cultures, CO_2 was dosed into the medium via conventional bubbles (approximately 3 mm in diameter) at a volumetric flow rate of nearly 5% V/V. CO_2 with 1%–5% mixture gas dosing along with the addition of certain concentration of carbonate in the medium, providing approximately 5–12 mM of equilibrium carbon concentration, could be employed to attain nearly 70–85% of the maximum growth potential and meanwhile to maintain the pH at a suitable range (7.0–7.5) for *H. pluvialis* growth (Ying et al., 2014). For the case of 5 L culture applying 1% CO_2 conventional dosing, the CO_2 mass transfer coefficient was estimated to be 5.6×10^{-5} min^{-1} in a preliminary experiment (data not shown), which could provide a maximal mass transfer rate of roughly 3.2×10^{-5} mol L^{-1} day^{-1} (Equation S8). This mass transfer

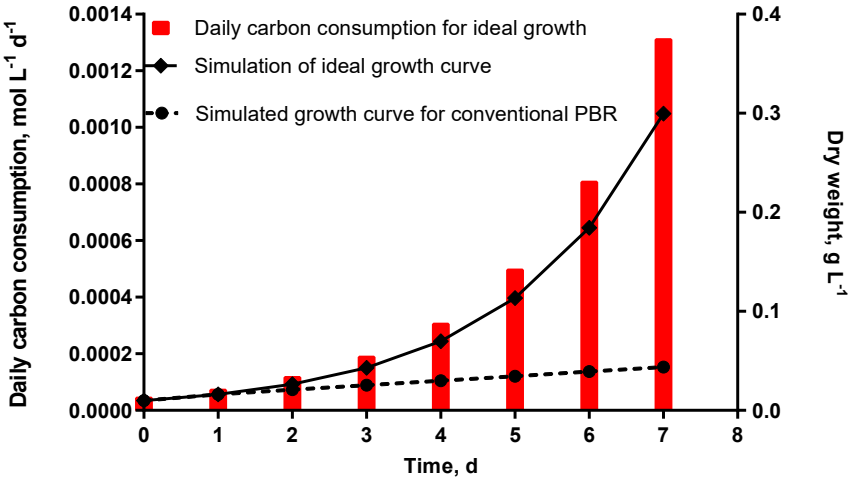

Figure 2. Simulated *H. pluvialis* growth at optimal specific growth rate and the daily carbon consumption

The dotted line stands for the simulation of the *H. pluvialis* growth in a conventional PBR culture, whereas the solid line with circles is the prediction of *H. pluvialis* growth under the circumstance that daily carbon supply meets or exceeds the consumption demand (Right Y axis). The bar demonstrates the daily carbon consumption (Left Y axis).

rate could only maintain *H. pluvialis* optimal growth for about 1 day. Thereafter, the *H. pluvialis* would grow linearly rather than exponentially (Figure 2).

The ideal growth scenario of *H. pluvialis* (at vegetative stage) along with its corresponding daily carbon consumption was then simulated based on this model, illustrated in Figure 2. Under the ideal conditions the *H. pluvialis* is expected to grow exponentially from initial 0.01 g L^{-1} to 0.30 g L^{-1} within 7 days, with the corresponding daily carbon consumption rising from about 4.4 × 10^{-5} mol L^{-1} day^{-1} to 1.3 × 10^{-3} mol L^{-1} day^{-1}. Therefore, to maintain the optimal growth for 7 days, the CO_2 mass transfer rate of 1.3 × 10^{-3} mol $L^{-1}d^{-1}$ is required according to a conservative consideration. The third part of this section will discuss a lab-scale experiment which has been done to validate the inference.

Mass transfer of microbubbles

The MDPBR designed based on chemical engineering

The CO_2 mass transfer efficiency is the main challenge to tackle. Since the CO_2 equilibrium concentration in the liquid depends on the partial pressure of CO_2 in the mixture gas (i.e. CO_2 volume percentage) according to Henry's law (Equation S8), the enhancement of K_La is crucial when the CO_2 volume percentage is fixed. The impact of KLa is analytically related to the mean bubble size (d_B) and the gas holdup (ε) (Erickson, 1990). To further clarify the gas holdup, it is defined as the volume fraction of gas in the gas-liquid dispersion (Najafpour, 2015), which is a function of bubble rising velocity (V_B), ratios of height to diameter (H/D), and liquid volume (V_L). According to Stokes' law, the mean value of the bubble rising velocity can be simplified as a function of liquid-gas density (ρ_L-ρ_G), viscosity (μ), bubble size (d_B) and gas flow rate (Q). After simplifications, our model was shown in Figure 4A, indicating that K_La is correlated to Q, H/D, VL, and d_B (Equation 4).

$$K_L\alpha = \frac{432\mu K_L}{\Pi(\rho_L-\rho_G)g\left(\frac{4}{\Pi}\right)^{\frac{2}{3}}}\cdot\frac{Q}{\left(\frac{V_L}{H/D}\right)^{\frac{2}{3}}d_B^3} = \alpha\frac{Q(H/D)^{\frac{2}{3}}}{V_L^{\frac{2}{3}}d_B^3} \qquad \text{Equation 4}$$

According to Equation 4, K_La is supposed to be in direct proportion to the item $Q(H/D)^{2/3}/(V_L{}^{2/3}d_B{}^3)$. Among those key parameters, bubble size has the most remarkable influence on mass transfer coefficient, followed by the gas flow rate. By individually increasing the Q and H/D by 10 times, the K_La could be improved by about 10 times and $10^{2/3}$ times, respectively, whereas the K_La could be 1000 times greater by reducing the bubble size by only 10 times.

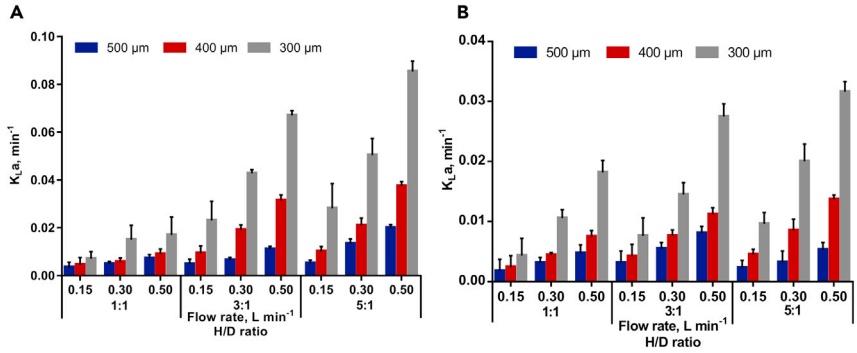

Figure 3. Measurement of CO_2 mass transfer coefficients

The CO_2 mass transfer coefficients in (A) 5 L and (B) 10 L water under different flow rates, H/D ratios, and bubble sizes. Owing to lab limitations, the error bars shown in this Figure were obtained from the triplication of each average bubble size under the conditions of 0.3 L min^{-1} dosing rate, 5 L liquid volume and 3:1 H/D ratio. Data points are presented as the mean ± standard deviation for triplicate measurements (n = 3).

The experimental results also support the correlation described in our model. Impacts of microbubble size, flow rate, H/D ratio, and liquid volume on CO_2 mass transfer were shown in Figure 3. Regarding bubble size (d_B), the K_La in different groups ranges from 0.0035 to 0.02 min^{-1}, 0.0045 to 0.0375 min^{-1}, and 0.007 to 0.0854 min^{-1} of 554 μm, 464 μm, or 333 μm bubble size respectively. In other words, when the bubble size was reduced by 40%, the K_La increased nearly 4 times. When it comes to flow rate (Q), increasing flow rate also leads to a higher gas hold-up (Ying et al., 2013a). In Figure 3A, by increasing flow rate from 0.15 to 0.5 L min^{-1}, the K_La almost tripled, rising from 0.007–0.03 min^{-1} to 0.02–0.09 min^{-1} with the H/D ratio of 5:1. In addition, increasing the H/D ratio can also enhance the K_La, as a longer bubble residence time in the liquid (Erickson, 1990). Nevertheless, the adjustment of H/D does not have the distinctive effect compared to the above parameters. For groups with microbubbles size of 333 μm at 0.5 L min^{-1}-flowrate, a 28.5% increase of K_La was observed after raising the H/D ratio 1.6 times.

On the other hand, the K_La values were reduced nearly by half when the liquid volume was doubled to 10 L (Figure 3B). Therefore, for scale-up cultures, flow rate, and H/D, the bubble size should be adjusted correspondingly to maintain the similar KLa desired for lab scale studies. Taken together, with the same liquid volume, K_La can be improved by either reducing the bubble sizes or increasing the flowrate and H/D ratio.

To further test the accuracy of the model, the theoretical data was compared with the practical data. The diagram of K_La versus the item $Q(H/D)^{2/3}/(V_L^{2/3}d_B^3)$ was plotted to find out the proportionality constant (α) in Equation 4 (Figure 4A). The linear regression with $R^2 = 0.89$ was obtained, indicating a strong proportional function between K_La and the item $Q(H/D)^{2/3}/(V_L^{2/3}d_B^3)$ (Figure 4B). The value of the proportionality constant α was determined to be 6×10^6. As shown in Figure 4C, the deviations of the major computational values are less than 30% in comparison with their corresponding practical values. To be concise, the deviations of half percentage of the data estimated are less than 20%. The main causes of deviation to the real values can be the occurrence of bubble coalescence, bubble entrainment, and internal turbulence, etc., which were not taken in consideration because of the simplifications.

Overall, our model (Equation 4) provided an archetype on the mathematical relationship between K_La and its relevant parameters. Based on the classic theory (such as two-film theory and stocks law) and the proportionality constant obtained from the practical trials, the model is reliable to predict K_La in the cultivation system. Hence, the mass transfer model built in this study could be used as guidance for the engineering design in the scale-up process.

Optimization of mass transfer parameters for H. pluvialis culture

To design the microbubble driven bioreactor, the K_La values were firstly estimated on three mean bubble sizes (350, 450, and 550 μm), four flow rates (0.05, 0.1, 0.15, and 0.3 L min^{-1}), and three H/D ratios (1, 3, 5) by using Equation 4. As discussed in previous section, for a 5 L lab-scale culture, CO_2 mass transfer rate of 1.3×10^{-3} mol $L^{-1}d^{-1}$ is required to maintain *H. pluvialis* optimal growth for 7 days, and to achieve a relatively high biomass density (around 0.3 g L^{-1} or 3×10^5 cells mL^{-1}). The estimated K_La ranged from

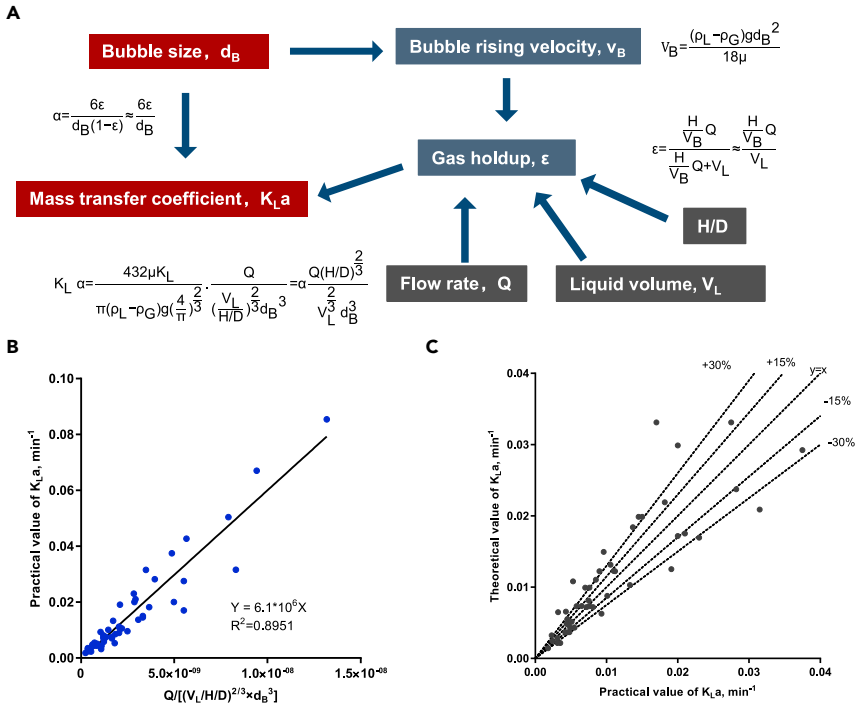

Figure 4. The mathematical relationship between K_La and its relevant parameters

(A) Schematic diagram demonstrating the relationship between mass transfer coefficient and its relevant parameters.

(B) plot of K_La versus the item $Q(H/D)^{2/3}/(V_L^{2/3}d_B^3)$. The K_La values were obtained from the experiments, while the values of the item $Q(H/D)^{2/3}/(V_L^{2/3}d_B^3)$ were calculated based on the practical values.

(C) the comparison between practical and theoretical values of K_La. The theoretical values of K_La were calculated using Equation 4.

0.61×10^{-3} min^{-1} to 0.042 min^{-1}, capable of achieving $0.35 \times 10^{-3} - 2.4 \times 10^{-2}$ mol $L^{-1}d^{-1}$ of mass transfer rate, under continuous 1% CO_2 dosing. We selected five sets of combinations (Table 2) which were close to the minimum carbon supply requirement. (The mass transfer rate of a 5 L-conventional bubble column PBR (Set. 6) with bubble size around 3 mm was also computed.) As mass production, energy consumption was considered. Higher flow rate means with the same amount of time and liquid volume, more gas was injected into the system which will create extra cost (Gil et al., 2010). Meanwhile, larger bubble sizes require lower injection pressure and less energy input (Han et al., 2002). Given energy cost and lower flow rate, larger bubble size (within the microbubble range) are favorable. Set. 5 requires both the smallest flow rate (0.05 L min^{-1}) and injection pressure, which well balances the mass transfer requirement with energy cost, and therefore was selected as the optimal combination of mass transfer parameters for 5 L-*H. pluvialis* culture.

Table 2. Estimations of mass transfer rates achievable under various combinations

No. of set	V_L, L	H/D	d_B, μm	Q, L min^{-1}	K_La, min^{-1} (10^{-3})	Daily mass transfer rate, mol L^{-1} day^{-1} (10^{-3})
1	5	1	350	0.05	2.4	1.4
2	5	1	450	0.1	2.3	1.3
3	5	3	450	0.05	2.3	1.4
4	5	3	550	0.1	2.6	1.5
5*	5	5	550	0.05	1.8	1.1
6	5	5	3000	0.25	0.056	0.032

Set.1-5 are the simulations for MDPBR, while Set.6 is the optimistic estimation for conventional PBR. The set being star marked was considered as optimal when balancing the mass transfer with energy cost.

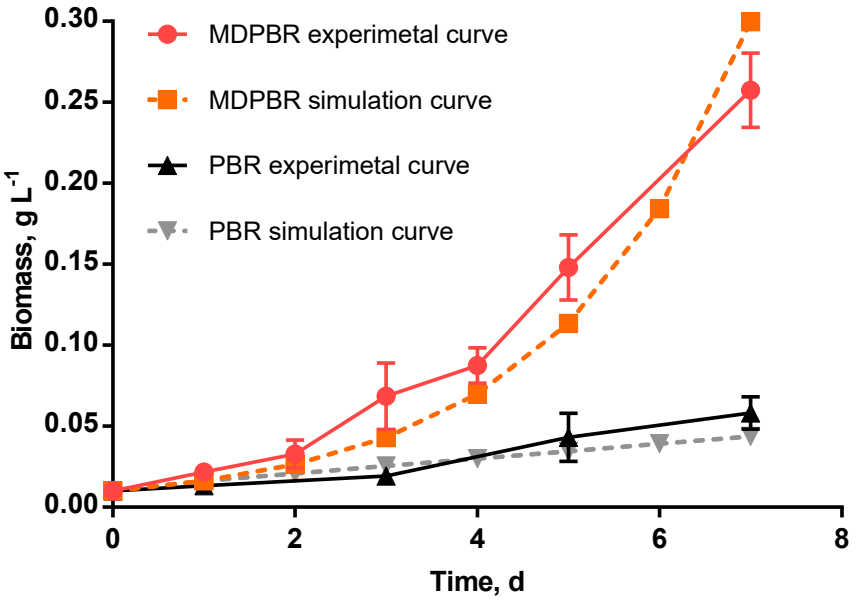

Figure 5. The biomass growth of *H. pluvialis* in both the conventional PBR and the MDPBR

The orange and gray dotted line represent the theoretical growth of *H. pluvialis* in the 5 L MDPBR and in the 5 L conventional PBR, respectively. The solid circle and triangle curves demonstrate the experimental data of *H. pluvialis* growth in the 5 L MDPBR and in the 5 L conventional PBR, respectively. Data points are presented as the mean ± standard deviation for triplicate measurements (n = 3).

H. pluvialis growth in an MDPBR

In our study, we demonstrated an optimized vision of conventional bubble column PBR. With airlift design (Figure S4) used to create proper circulation, a microbubble technique was harnessed to improve carbon supply at a relatively low energy cost.

We designed a 5 L MDPBR which was capable of generating nearly 550 μm microbubbles in comparison with conventional PBR which generates around 3 mm bubbles for *H. pluvialis* culture. The gas flow rates were set to be 0.05 L min^{-1} and 0.25 L min^{-1} for the former and later, respectively. The results were shown in Figure 5. Generally, the dry weight of *H. pluvialis* cultured in the MDPBR increased by nearly 30 times at the end of a week, with an overall specific growth rate was relatively close to the optimal value 0.49 d^{-1} as expected and the exponential growth was maintained up to the seventh day. Almost all the cells were confirmed to be vegetative at the final day of cultivation via microscope observation (Figure S6). It was therefore confirmed that our MDPBR can maintain the optimal growth of *H. pluvialis* under proper light intensity. Besides, the experimental data were found to be almost consistent with the simulated data, which confirmed the reliability of the experimental data as well as the validity of the kinetic model for *H. pluvialis* growth in Table 1. In comparison, the *H. pluvialis* in the conventional PBR grew linearly instead of exponentially and achieved 0.21 d^{-1} of specific growth rate with only about 0.06 g L^{-1} of final biomass concentration, whereas the MDPBR achieved approximately 5 times higher biomass concentration (0.3 g L^{-1}), with only 1/5 of gas flow rate. The results suggest that the MDPBR could be 25 times more efficient than the conventional PBR, in terms of output-input ratio.

CONCLUSION

In this study, the CO_2 demand of maintaining *H. pluvialis* exponential growth was profiled, implying insufficient carbon supply through the traditional bubble system. To meet the demand, a novel MDPBR was proposed to facilitate mass transfer through minimizing bubble size. Our hypothesis of CO_2 supply and *H. pluvialis* growth has been validated via a cultivation trial in MDPBR, in which a significant improvement (5 times higher) of the *H. pluvialis* biomass productivity has been achieved with reduction in power consumption. Furthermore, our previous work (Wu et al., 2020) which applied higher light intensity suggested that our MDPBR has a potential of reaching higher biomass than that has been achieved so far. This technology offers an efficient alternative for *H. pluvialis* mass production and could further serve as a useful tool for CO_2 mitigation and bioproduct production.

Limitations of the study

This study designed MDPBR for *H. pluvialis* massive growth, and the CO_2 capture ability of *H. pluvialis* has been proved. However, the light intensity in this study may not be optimal for maximum photosynthesis, in terms of CO_2 supply. The stabilities and efficiency of MDPBR should be especially followed with interests and improved for the practical applications. The CO_2 supply can maintain a 7-day log growth so far; nevertheless, MDPBR can be adapted to exploit higher algal productivity in industrialized production. For the astaxanthin induction stage, whether acetate addition or increasing CO_2 supply will benefit astaxanthin accumulation can be further explored.

STAR★METHODS

Detailed methods are provided in the online version of this paper and include the following:

- KEY RESOURCES TABLE
- RESOURCE AVAILABILITY
  - Lead contact
  - Materials availability
  - Data and code availability
- EXPERIMENTAL MODEL AND SUBJECT DETAILS
- METHOD DETAILS
  - Growth and carbon consumption kinetics
  - Mass transfer tests
  - Microbubble-driven photobioreactor culture
- QUANTIFICATION AND STATISTICAL ANALYSIS

SUPPLEMENTAL INFORMATION

Supplemental information can be found online at https://doi.org/10.1016/j.isci.2021.103461.

ACKNOWLEDGMENTS

This work was financially supported by the S&T Projects of the Economic, Trade and Information Commission of Shenzhen (No. 20180124085935704), Guangdong Basic and Applied Basic Research Foundation (2020B1515120012), as well as the S&T Projects of Shenzhen Science and Technology Innovation Committee (JCYJ20200109142822787, JCYJ20200109142818589, and RCJC20200714114433069).

AUTHOR CONTRIBUTIONS

Kebi Wu, Kezhen Ying, Jin Zhou, Yi Tao and Zhonghua Cai designed the research. Kezhen Ying, Kebi Wu and Dai Liu, Lu Liu conducted the experiments. Kebi Wu and Kezhen Ying drafted the manuscript and analyzed the data. Jin Zhou, Yi Tao, Xiaoshan Zhu and Zhonghua Cai contributed to the critical revision of the article. James Hanotu provided an editorial service.

DECLARATION OF INTERESTS

There is no conflict of interest, informed consent, human, animal rights applicable or Chinese patent (ZL201810168432.1). All authors agreed to the authorship and the submission of the manuscript for peer review.

Received: April 24, 2021
Revised: September 26, 2021
Accepted: November 11, 2021
Published: December 17, 2021

REFERENCES

Aflalo, C., Meshulam, Y., Zarka, A., and Boussiba, S. (2007). On the relative efficiency of two- vs. one-stage production of astaxanthin by the green alga *Haematococcus pluvialis*. Biotechnol. Bioeng. *98*, 300–305.

Agranat, O. (2007). Optimization of Inorganic Carbon Sources in Open Pond Cultures of *Haematococcus pluvialis* (Ben Gurion University).

Ambati, R.R., Phang, S.-M., Ravi, S., and Aswathanarayana, R.G. (2014). Astaxanthin: sources, extraction, stability, biological activities and its commercial applications—a review. Mar. Drugs *12*, 128–152.

Borowiak, D., Lenartowicz, P., Grzebyk, M., Wiśniewski, M., Lipok, J., and Kafarski, P. (2021). Novel, automated, semi-industrial modular photobioreactor system for cultivation of demanding microalgae that produce fine chemicals—the next story of *H. pluvialis* and astaxanthin. Algal Res. *53*, 102151.

Burgess, S.J., Tamburic, B., Zemichael, F., Hellgardt, K., and Nixon, P.J. (2011). In Chapter 3 - Solar-Driven Hydrogen Production in Green Algae, Advances in Applied Microbiology, A.I. Laskin, S. Sariaslani, and G.M. Gadd, eds. (Academic Press), pp. 71–110.

Chan, K.-C., Pen, P.-J., and Yin, M.-C. (2012). Anticoagulatory and antiinflammatory effects of astaxanthin in diabetic rats. J. Food Sci. *77*, 76–80.

Choi, Y.Y., Joun, J.M., Lee, J., Hong, M.E., Pham, H.-M., Chang, W.S., and Sim, S.J. (2017). Development of large-scale and economic pH control system for outdoor cultivation of microalgae *Haematococcus pluvialis* using industrial flue gas. Bioresour. Technol. *244*, 1235–1244.

Colusse, G.A., Duarte, M.E.R., de Carvalho, J.C., and Noseda, M.D. (2021). In Chapter 7 - Production of Astaxanthin by Haematococcus pluvialis: Lab Processes to Scale up Including the Cost Considerations, Global Perspectives on Astaxanthin, G.A. Ravishankar and A. Ranga Rao, eds. (Academic Press), pp. 121–130.

Ding, D., Chen, S., Peng, S., Jiang, C., Zheng, L., and Li, J. (2019). Strategies of phosphorus utilization in an astaxanthin-producing green alga *Haematococcus pluvialis*, a comparison with a bloom-forming cyanobacterium Microcystis wesenbergii. Aquat. Ecol. *53*, 679–688.

Dodds, W.K. (2002). In Carbon, Freshwater Ecology, W.K. Dodds, ed. (Academic Press), pp. 229–244.

Dodds, W.K., and Whiles, M.R. (2010). In Carbon, Freshwater Ecology, Second Edition, W.K. Dodds and M.R. Whiles, eds. (Academic Press), pp. 323–343.

Erickson, L.E. (1990). Airlift Bioreactors (Elsevier Applied Science).

Fakhri, S., Nouri, Z., Moradi, S.Z., and Farzaei, M.H. (2020). Astaxanthin, COVID-19 and immune response: focus on oxidative stress, apoptosis and autophagy. Phytother. Res. *34*, 2790–2792.

García-Malea, M.C., Acién, F.G., Fernández, J.M., Cerón, M.C., and Molina, E. (2006). Continuous production of green cells of *Haematococcus pluvialis*: modeling of the irradiance effect. Enzyme Microb. Technol. *38*, 981–989.

Gil, J.A., Túa, L., Rueda, A., Montaño, B., Rodríguez, M., and Prats, D. (2010). Monitoring and analysis of the energy cost of an MBR. Desalin *250*, 997–1001.

Gunjal, P.R., and Ranade, V.V. (2016). In Chapter 7 - Catalytic Reaction Engineering, Industrial Catalytic Processes for Fine and Specialty Chemicals, S.S. Joshi and V.V. Ranade, eds. (Elsevier), pp. 263–314.

Gupta, P.L., Lee, S.-M., and Choi, H.-J. (2015). A mini review: photobioreactors for large scale algal cultivation. World J. Microbiol. Biotechnol. *31*, 1409–1417.

Han, M., Park, Y., Lee, J., and Shim, J. (2002). Effect of pressure on bubble size in dissolved air flotation. Water Supply *2*, 41–46.

Hillebrand, H., and Sommer, U. (1999). The nutrient stoichiometry of benthic microalgal growth: redfield proportions are optimal. Limnol. Oceanogr. *44*, 440–446.

Huang, D., Liu, W., Li, A., Hu, Z., Wang, J., and Wang, C. (2021). Cloning and identification of a novel β-carotene hydroxylase gene from *Haematococcus pluvialis* and its function in Escherichia coli. Algal Res. *55*, 102245.

Jerney, J., and Spilling, K. (2020). In Large Scale Cultivation of Microalgae: Open and Closed Systems, Biofuels from Algae: Methods and Protocols, K. Spilling, ed. (Springer New York), pp. 1–8.

Judd, S.J., Al Momani, F.A.O., Znad, H., and Al Ketife, A.M.D. (2017). The cost benefit of algal technology for combined CO_2 mitigation and nutrient abatement. Renew. Sustain. Energy Rev. *71*, 379–387.

Kadic, E., and Heindel, T.J. (2014). In Stirred-Tank Bioreactors, an Introduction to Bioreactor Hydrodynamics and Gas-Liquid Mass Transfer, E. Kadic and T.J. Heindel, eds. (John Wiley & Sons, Inc), pp. 69–123.

Kaewpintong, K., Shotipruk, A., Powtongsook, S., and Pavasant, P. (2007). Photoautotrophic high-density cultivation of vegetative cells of *Haematococcus pluvialis* in airlift bioreactor. Bioresour. Technol. *98*, 288–295.

Kampen, W.H. (2014). In Chapter 4 - Nutritional Requirements in Fermentation Processes, Fermentation and Biochemical Engineering Handbook, Third Edition, H.C. Vogel and C.M. Todaro, eds. (William Andrew Publishing), pp. 37–57.

Kang, C.D., Lee, J.S., Park, T.H., and Sim, S.J. (2005). Comparison of heterotrophic and photoautotrophic induction on astaxanthin production by *Haematococcus pluvialis*. Appl. Microbiol. Biotechnol. *68*, 237–241.

Kazakis, N.A., Mouza, A.A., and Paras, S.V. (2008). Experimental study of bubble formation at metal porous spargers: effect of liquid properties and sparger characteristics on the initial bubble size distribution. Chem. Eng. J. *137*, 265–281.

Khoo, K.S., Lee, S.Y., Ooi, C.W., Fu, X., Miao, X., Ling, T.C., and Show, P.L. (2019). Recent advances in biorefinery of astaxanthin from Haematococcus pluvialis. Bioresour. Technol. *288*, 121606.

Kim, H.-Y., Kim, Y.-M., and Hong, S. (2019). Astaxanthin suppresses the metastasis of colon cancer by inhibiting the MYC-mediated downregulation of microRNA-29a-3p and microRNA-200a. Sci. Rep. *9*, 9457.

Le-Feuvre, R., Moraga-Suazo, P., Gonzalez, J., Martin, S.S., Henríquez, V., Donoso, A., and Agurto-Muñoz, C. (2020). Biotechnology applied to *Haematococcus pluvialis* Fotow: challenges and prospects for the enhancement of astaxanthin accumulation. J. Appl. Phycol. *32*, 3831–3852.

Lee, J.Y., Hong, M.-E., Chang, W.S., and Sim, S.J. (2015). Enhanced carbon dioxide fixation of *Haematococcus pluvialis* using sequential operating system in tubular photobioreactors. Process. Biochem. *50*, 1091–1096.

Liu, X., Ying, K., Chen, G., Zhou, C., Zhang, W., Zhang, X., Cai, Z., Holmes, T., and Tao, Y. (2017). Growth of *Chlorella vulgaris* and nutrient removal in the wastewater in response to intermittent carbon dioxide. Chemosphere *186*, 977–985.

Medhi, J., and Kalita, M.C. (2021). Astaxanthin: an algae-based natural compound with a potential role in human health-promoting effect: an updated comprehensive review. J. Appl. Biol. Biotechnol. *9*, 114–123.

Nagappan, S., Devendran, S., Tsai, P.-C., Dahms, H.-U., and Ponnusamy, V.K. (2019). Potential of two-stage cultivation in microalgae biofuel production. Fuel *252*, 339–349.

Nahidian, B., Ghanati, F., Shahbazi, M., and Soltani, N. (2018). Effect of nutrients on the growth and physiological features of newly isolated *Haematococcus pluvialis* TMU1. Bioresour. Technol. *255*, 229–237.

Najafpour, G. (2015). Chapter 5 - Growth Kinetics, Biochemical Engineering and Biotechnology, Second Edition (Elsevier), pp. 127–192.

Olaizola, M. (2000). Commercial production of astaxanthin from *Haematococcus pluvialis* using 25,000-liter outdoor photobioreactors. J. Appl. Phycol. *12*, 499–506.

Pan-utai, W., Parakulsuksatid, P., and Phomkaivon, N. (2017). Effect of inducing agents on growth and astaxanthin production in *Haematococcus pluvialis*: organic and inorganic. Biocatal. Agric. Biotechnol. *12*, 152–158.

Oslan, S.N., Shoparwe, N.F., Yusoff, A.H., Rahim, A.A., Chang, C.S., Tan, J.S., Oslan, S.N., Arumugam, K., Ariff, A.B., Sulaiman, A.Z., and Mohamed, M.S. (2021). A review on haematococcus pluvialis bioprocess optimization of green and red stage culture conditions for the production of natural astaxanthin. Biomolecules *11*, 1–15.

Pang, N., and Chen, S. (2017). Effects of C5 organic carbon and light on growth and cell activity of *Haematococcus pluvialis* under mixotrophic conditions. Algal Res. *21*, 227–235.

Panis, G., and Carreon, J.R. (2016). Commercial astaxanthin production derived by green alga *Haematococcus pluvialis*: a microalgae process model and a techno-economic assessment all through production line. Algal Res. *18*, 175–190.

Perdue, E.M. (2009). In Natural Organic Matter, Encyclopedia of Inland Waters, G.E. Likens, ed. (Academic Press), pp. 806–819.

Razon, L.F. (2011). In Net Energy Calculations for Production of Biodiesel and Biogas from Haematococcus pluvialis and Nannochloropsis sp, Zero-Carbon Energy Kyoto 2010, T. Yao, ed. (Springer Japan), pp. 83–91.

Redfield, A., Ketchum, B., and Richards, F. (1963). In The Influence of Organisms on the Composition of Seawater, The Sea, M.N. Hill, ed. (Harvard University Press), pp. 26–77.

Rehman, F., Medley, G.J.D., Bandulasena, H., and Zimmerman, W.B.J. (2015). Fluidic oscillator-mediated microbubble generation to provide cost effective mass transfer and mixing efficiency to the wastewater treatment plants. Environ. Res. *137*, 32–39.

Ryu, H.J., Oh, K.K., and Kim, Y.S. (2009). Optimization of the influential factors for the improvement of CO_2 utilization efficiency and CO_2 mass transfer rate. J. Ind. Eng. Chem. *15*, 471–475.

Sarada, R., Tripathi, U., and Ravishankar, G.A. (2002). Influence of stress on astaxanthin production in *Haematococcus pluvialis* grown under different culture conditions. Process. Biochem. *37*, 623–627.

Schultze, L.K.P., Simon, M.-V., Li, T., Langenbach, D., Podola, B., and Melkonian, M. (2015). High light and carbon dioxide optimize surface productivity in a twin-layer biofilm photobioreactor. Algal Res. *8*, 37–44.

Singh, S.K., Rahman, A., Dixit, K., Nath, A., and Sundaram, S. (2016). Evaluation of promising algal strains for sustainable exploitation coupled with CO_2 fixation. Environ. Technol. *37*, 613–622.

Talukdar, J., Bhadra, B., Dattaroy, T., Nagle, V., and Dasgupta, S. (2020). Potential of natural astaxanthin in alleviating the risk of cytokine storm in COVID-19. Biomed. Pharmacother. *132*, 110886.

Tocquin, P., Fratamico, A., and Franck, F. (2012). Screening for a low-cost *Haematococcus pluvialis* medium reveals an unexpected impact of a low N/P ratio on vegetative growth. J. Appl. Phycol. *24*, 365–373.

Wan, M., Zhang, J., Hou, D., Fan, J., Li, Y., Huang, J., and Wang, J. (2014). The effect of temperature on cell growth and astaxanthin accumulation of *Haematococcus pluvialis* during a light–dark cyclic cultivation. Bioresour. Technol. *167*, 276–283.

Wang, X., Miao, X., Chen, G., Cui, Y., Sun, F., Fan, J., Gao, Z., and Meng, C. (2021). Identification of microRNAs involved in astaxanthin accumulation responding to high light and high sodium acetate (NaAC) stresses in *Haematococcus pluvialis*. Algal Res. *54*, 102179.

Wen, X., Wang, Z., Ding, Y., Geng, Y., and Li, Y. (2020). Enhancing the production of astaxanthin by mixotrophic cultivation of *Haematococcus pluvialis* in open raceway ponds. Aquacult. Int. *28*, 625–638.

Wu, K., Ying, K., Liu, L., Zhou, J., and Cai, Z. (2020). High irradiance compensated with CO_2 enhances the efficiency of *Haematococcus lacustris* growth. Biotechnol. Rep. *26*, e00444.

Xi, T., Kim, D.G., Roh, S.W., Choi, J.-S., and Choi, Y.-E. (2016). Enhancement of astaxanthin production using *Haematococcus pluvialis* with novel LED wavelength shift strategy. Appl. Microbiol. Biotechnol. *100*, 6231–6238.

Yao, K., Chi, Y., Wang, F., Yan, J., Ni, M., and Cen, K. (2016). The effect of microbubbles on gas-liquid mass transfer coefficient and degradation rate of COD in wastewater treatment. Water Sci. Technol. *73*, 1969–1977.

Ying, K., Al-Mashhadani, M.K.H., and Hanotu, J.O. (2013a). Enhanced mass transfer in microbubble-driven airlift bioreactor for microalgal culture. Engineering *5*, 1947–3931.

Ying, K., Gilmour, D.J., Shi, Y., and Zimmerman, W.B. (2013b). Growth enhancement of *Dunaliella salina* by microbubble induced airlift loop bioreactor (ALB)—the relation between mass transfer and growth rate. J. Biomater. Nanobiotechnol. *4*, 1–9.

Ying, K., Zimmerman, W., and Gilmour, D. (2014). Effects of CO_2 and pH on growth of the microalga *Dunaliella salina*. J. Microb. Biochem. Technol. *6*, 167–173.

Zhang, X.W., Gong, X.-D., and Chen, F. (1999). Kinetic models for astaxanthin production by high cell density mixotrophic culture of the microalga *Haematococcus pluvialis*. J. Ind. Microbiol. Biotechnol. *23*, 691–696.

Zhao, Y., Hou, Y., Chai, W., Liu, Z., Wang, X., He, C., Hu, Z., Chen, S., Wang, W., and chen, F. (2020). Transcriptome analysis of *Haematococcus pluvialis* of multiple defensive systems against nitrogen starvation. Enzyme Microb. Technol. *134*, 109487.

Zimmerman, W.B., Zandi, M., Hemaka Bandulasena, H.C., Tesař, V., James Gilmour, D., and Ying, K. (2011). Design of an airlift loop bioreactor and pilot scales studies with fluidic oscillator induced microbubbles for growth of a microalgae *Dunaliella salina*. Appl. Energy. *88*, 3357–3369.

STAR★METHODS

KEY RESOURCES TABLE

REAGENT or RESOURCE	SOURCE	IDENTIFIER
Experimental models: Organisms/strains		
H. pluvialis: FACHB-712	Culture Collection of Algae at Chinese Academy of Sciences	FACHB-712
Chemicals, peptides, and recombinant proteins		
Bold's basal medium	Culture Collection of Algal and Protozoa, Scottish Marine Institute, UK	https://www.ccap.ac.uk/wp-content/uploads/MR_BB.pdf
Software and algorithms		
CO_2 mass transfer efficiency	This paper (Equation 4)	NA
Total carbon concentration	This paper (Equation S7)	NA
ImageJ	Version 1.8.0	https://imagej.nih.gov/ij/download.html
Prism - GraphPad	Version 7.0	https://www.graphpad.com/scientific-software/prism/
SPSS	version 20.0	https://www.ibm.com/support/pages/downloading-ibm-spss-statistics-20
Other		
ZEISS primovert light microscopes	Carl Zeiss AG	https://www.zeiss.com/microscopy/us/products/light-microscopes.html
pH meter	Mettler Toledo	FiveEasy Plus 28
Ceramic diffusers	Zibo Wastewater Treatment Technology Co. Ltd.	NA
Luminometer	Onset Computer Corporation	HOBO-Temp/Light MX2202

RESOURCE AVAILABILITY

Lead contact

Further information and requests for resources should be directed to and will be fulfilled by the lead contact, Prof. Zhonghua Cai (caizh@sz.tsinghua.edu.cn).

Materials availability

Not applicable.

Data and code availability

Cell growth and bioreactor parament data reported in this paper will be shared by the lead contact upon request. This paper does not report original code.

EXPERIMENTAL MODEL AND SUBJECT DETAILS

H. pluvialis FACHB-712 was obtained from the Culture Collection of Algae at Chinese Academy of Sciences and maintained in the BBM medium suggested by CCAP (Culture Collection of Algal and Protozoa, Scottish Marine Institute, UK). Culture temperature was maintained at 25–26°C.

METHOD DETAILS

Growth and carbon consumption kinetics

To investigate the impact of carbon concentration on *H. pluvialis* growth (referring particularly to the growth at vegetative phase) as well as the kinetics of growth and carbon consumption, 250 mL-Duran bottles containing 140 mL of BBM medium each were prepared for the experiment (Figure S1).

The primarily inorganic carbon in the atmosphere is CO_2, while in water body, inorganic carbon concentration is defined as the sum of all different forms (Dodds and Whiles, 2010):

Under experimental condition, gaseous and bicarbonate (HCO_3^-) is the major form of CO_2 in the medium the pH of which is around 7–8 (Dodds, 2002). To avoid the gas exchange of atmospheric CO_2, and ensure the carbon supply, a bicarbonate solution was used to elaborate the consumption kinetics.

For every three Duran bottles, different amount of $NaHCO_3$ were added to make the final carbon concentration at 2 mM, 4 mM, and 8 mM, respectively. 10 mL of *H. pluvialis* at exponential growth phase (with concentration of about 7.5×10^5 cells mL^{-1}) was inoculated to each bottle.

According to previous studies, as a light sensitive species the optimal lighting has been reported as 20 μmol photo $m^{-2}s^{-1}$(Kaewpintong et al., 2007) and for the first stage cultivation, studies has been carried on under illumination of 20–25 μmol $m^{-2}s^{-1}$(Ding et al., 2019; Huang et al., 2021). Hence, it is suitable to use 20 μmol photo $m^{-2}s^{-1}$ cultivation condition for energy saving concerns. Continuous illumination was provided by the LED white light at the intensity of 20 μmol photo $m^{-2}s^{-1}$. Culture temperature was maintained at the room temperature (25–26°C). pH value at 7–8 was widely considered to favorite the vegetative cultivation(Borowiak et al., 2021; Choi et al., 2017).The pH value was sustained at 7–8 with HCO_3^-/CO_2 buffer system.

To ensure that the carbon concentration was the only limiting factor, the cultivation was only lasted for 36 h to minimize the effects of light attenuation and nutrients depletion when the culture became denser. The experiment was run in triplicate. The biomass and carbon concentrations were measured every 12 h. Except for the sampling period, each Duran bottle was sealed tight for almost the entire culture period to maximally prevent the CO_2 loss to the atmosphere. Besides, a separate set of Duran bottles containing 2 mM, 4 mM, and 8 mM of total carbon in the same BBM medium but without inoculating *H. pluvialis* was applied as the blank control to offset the CO_2 loss during the sampling period. The cell counts were conducted through microscopy. A standard curve between cell counts and dry weight was established via a preliminary experiment. The average dry weight per cell was found to be 1×10^{-9}g, which was identical to the value reported by others (Olaizola, 2000). Therefore, the dry biomass in this study was estimated based on the cell counts. The total inorganic carbon concentration (C_T) was measured by the Elemental Analyzer (Flash 2000 HT). To be noted, the 'carbon concentration' mentioned all through the text refers to the total inorganic carbon concentration, including dissolved CO_2, HCO_3^- and CO_3^{2-}.

Regarding the kinetics, the overall specific growth rate (μ′, d^{-1}) for a certain period was calculated through Equation S1,

$$\mu' = (\ln W_2 - \ln W_1)/(t_2 - t_1) \quad \text{Equation S1}$$

where W_2 and W_1 are the biomass dry weight (g L^{-1}) at time t_2 and t_1, separately.

The rate of biomass production is represented by Equation S2, of which the integration form is presented as Equation S3,

$$\frac{dW}{dt} = \mu \cdot W \quad \text{Equation S2}$$

$$W = W_0 e^{\mu t} \quad \text{Equation S3}$$

where dW/dt is the instantaneous growth rate (g L^{-1} day^{-1}), μ is the instantaneous specific growth rate (d^{-1}), W and W_0 mean the instantaneous and initial biomass concentration (g L^{-1}), separately. t is the time of cultivation. While the instantaneous specific growth rate μ (d^{-1}) can be estimated using Monod equation (Equation 1).

Based on substrate consumption model(Zhang et al., 1999), the consumption rate of carbon (dC_C/dt, mol L^{-1} day^{-1}) is described as Equation S4, its integration form Equation S5 represents the total amount of carbon ($\triangle C_C$, mol L^{-1}) consumed by microalgae within a certain period,

$$\frac{dC_C}{dt} = \frac{\mu \cdot W}{Y_{W/C}} = \frac{\mu \cdot W_0 e^{\mu t}}{Y_{W/C}} \quad \text{Equation S4}$$

$$\Delta C_C = \frac{W_0}{Y_{W/C}}(e^{\mu t} - 1) \quad \text{Equation S5}$$

where $Y_{W/C}$ is the yield coefficients based on carbon (g mol^{-1}).

The residual concentrations of carbon (C_C, mol L^{-1}) is calculated via Equation S6,

$$C_C = C_{C0} - \Delta C_C = C_{C0} - \frac{W_0}{Y_{W/C}}(e^{\mu t} - 1) \quad \text{Equation S6}$$

The key coefficients/constants for the kinetics model including the maximum growth rate (μ_{max}), yield coefficient on carbon ($Y_{W/C}$), the half saturation constant of carbon (K_C) were obtained via graphic methods, which were demonstrated by our previous work (Liu et al., 2017).

Mass transfer tests

To study the CO_2 mass transfer property of microbubbles as well as the impacts of the relevant parameters on it, two practical volumes of reactor (V_{ol}), three ratios of height to diameter (H/D), three average microbubble sizes (d_B) and three flowrates (Q) were selected for K_La (mass transfer coefficient) tests (Figure S2). Six airlift bioreactors with two working volumes (5 L and 10 L) and three H/D ratios (1:1, 3:1 and 5:1), made of PMMA, were customized from Hongxing Machinery Co. Ltd. (Ningbo, Zhejiang, China). For each reactor, there was a replaceable diffuser housing fixed at the bottom to allow switching the diffusers. Microbubbles with average sizes (d_{32}) of 333 μm, 464 μm, and 554 μm were generated from three types of ceramic diffusers specifically customized by Zibo Wastewater Treatment Technology Co. Ltd. (Zibo, Shangdong, China). Here, the average bubble diameters were characterized using a high-speed camera via a separate experiment. Bubbles were generated by injecting 5% CO_2 mixture gas through the ceramic diffuser placing at the bottom of a transparent fish tank. The gas flowrate was set to be 0.1 L min^{-1}. A tripod halogen floodlight was adjusted to a proper position to illuminate the bubbles. A high-speed camera connected to a computer was placed in front of the fish tank to visualize the bubbles, and a black paper was attached to the back of the fish tank, making the bubbles easier to be visualized. The captured bubble images were then analyzed by a software 'ImageJ'.

For each mass transfer test, 5% CO_2 mixture gas (balanced with N_2) provided by a gas cylinder was injected into the reactor containing a certain volume of deionized water. The flowrate was measured by a flow meter fixed in between the inlet of the diffuser and the outlet of the gas cylinder. Three gas flowrates (0.15, 0.3 and 0.5 L min^{-1}) were applied in this experiment. The pH value was recorded every 30 s, measured by a pH meter (FiveEasy Plus 28). The total carbon concentration (C_T) was calculated based on the pH value by using Equation S8 reported in Ying et al. (Ying et al., 2013a, 2013b),

$$[C_T] = \left(1 + 10^{pH-6.381} + 10^{2pH-16.758}\right)\frac{\left(10^{-pH} - 10^{pH-14} + Na^+\right)10^{-2pH}}{10^{-6.381-pH} + 2 \times 10^{-16.758}} \quad \text{Equation S7}$$

where Na^+ specifically means the concentration of sodium (mol L^{-1}) for the sodium bicarbonate added.

The CO_2 mass transfer coefficient K_La for each test was determined via the graphic method interpreted by Chisti (Erickson, 1990; Ying et al., 2013a). The mass transfer rate (dC/dt) can be described in Equation S9, where C represents the concentration of total dissolved carbon while C* is the equilibrium/saturation concentration. Its integration form can be written as Equation S9, where t stands for time, C_t and C_0 are the instantaneous concentration and initial concentration of total dissolved carbon, respectively. By plotting ln [(C* - C_0)/(C* - C_t)] versus t, a linear regression is easily tractable, where the slope value equals to the K_La.

$$\frac{dC}{dt} = K_La(C* - C) \quad \text{Equation S8}$$

$$ln\frac{C* - C_0}{C* - C_t} = K_La \cdot t \quad \text{Equation S9}$$

Microbubble-driven photobioreactor culture

The cultivation was conducted adopting typical two-stage mode. At the vegetative growth stage, *H. pluvialis* were cultured in an MDPBR with suitable illumination for one week (Figure S3). At the second stage, the algal broth was transferred into several flasks for astaxanthin induction under higher irradiance. Since this study has mainly focused on *H. pluvialis* vegetative growth, so the detailed information about

astaxanthin accumulation at second stage was not mentioned. Figure S4 showed the set-up for a 5 L lab trial. 200 mL of *H. pluvialis* growing at exponential growth phase was added to a customized MDPBR containing 5 L BBM medium. The H/D ratio of the MDPBR was 5:1. 1% CO_2 mixture gas was continuously dosed into the MDPBR at 0.05 L min^{-1}, with the microbubbles generated at an average size of 550 μm. The key parameters here regarding to reactor geometry and microbubbles, including height, diameter, bubble size and gas flow rate, were specifically determined. An additional 5 mM of sodium bicarbonate was included in the BBM medium, maintaining the pH at around 7.5 for the entire culture period under constant CO_2 bubbling. Two of fluorescence lamps providing continuous illumination were fixed at the side of MDPBR using iron stands. As *H. pluvialis* started to grow, the light attenuation occurred simultaneously, so the number of fluorescence lamps was doubled after 3 days to maintain a sufficient illumination. As a result, the light intensity at the reactor center was kept at around 16–20 μmol photo m^{-2} s^{-1} during the whole culture period, measured by a luminometer (HOBO-Temp/Light MX2202, Onset Computer Corporation) immerging into the algal broth. 5 mL of sample was taken each day for the measurement of growth. A control experiment was also conducted in a 5 L conventional PBR with the same geometry settings. The gas sparger generating bubbles with approximately 3 mm in diameter was employed at the bottom of the PBR. To maintain a sufficient mixing, the flowrate of 5% V/V (i.e. 0.25 L min^{-1}) was applied in the control experiment. The other parameters were set as the same as for the MDPBR.

QUANTIFICATION AND STATISTICAL ANALYSIS

The data were processed by one-way analysis of variance using SPSS version 20.0 (SPSS, USA) and Prism-GraphPad version 7.0. The average value of three replicate samples was expressed as mean ± standard deviation. A value of $P < 0.05$ was considered statistically significant.